

# IN-PLANE DIMENSIONAL STABILITY OF THREE-LAYER ORIENTED STRANDBOARD<sup>1</sup>

*Jong N. Lee*<sup>†</sup>

Postdoctoral Researcher

and

*Qinglin Wu*<sup>†</sup>

Associate Professor

Louisiana Forest Products Laboratory  
School of Forestry, Wildlife, and Fisheries  
Louisiana State University Agricultural Center  
Baton Rouge, LA 70803-6202

(Received November 2000)

## ABSTRACT

In-plane swelling and bending properties of three-layer oriented strandboard (OSB) were investigated under the interactive influence of flake alignment level (FAL), flake weight ratio (FWR), resin content (RC), vertical density gradient, and moisture content (MC) levels. Mathematical models based on lamination theories were developed to predict effective modulus (EM), linear expansion (LE), and internal swelling stresses. The model's prediction was compared with actual experimental data.

It was shown that the relationship between LE and MC change for OSB was curvilinear with larger expansion rates at lower MC levels. FAL and FWR were two primary variables that significantly affected the magnitudes of LE, modulus of elasticity (MOE), and modulus of rupture (MOR). Increase in RC from 4% to 6% led to little change in all three properties.

The model predicted general trends of change in LE, EM, and swelling stresses as a function of FWR at the two alignment and two RC levels. The model's prediction in both EM and LE compared favorably with the experimental data. Prediction of the in-plane swelling stresses showed the effect of the panel MC change and directional dependency. The model provides an analytical tool for optimizing flake alignment level and panel flake weight ratio to achieve a proper balance between EM and LE for OSB manufacturing.

*Keywords:* Effective modulus, linear expansion, modeling, panel design, processing variables, structural panel.

## INTRODUCTION

Dimensional stability is an important property in the use of oriented strandboard (OSB). Special attention to dimensional stability of wood-based materials has always been demanded since changes in the relative humidity (RH) of the surrounding atmosphere can affect their unit dimensions to a much greater extent than the thermo-effects that control dimensional changes in nonhygroscopic materials

(Bryan 1962). Out-of-plane swelling, known as thickness swelling (TS), is often accompanied by permanent strength loss and sometimes product failure. It has been widely studied by Jorgensen and Odell (1961), Johnson (1964), Halligan (1970), Halligan and Schniewind (1974), Lehmann (1978), Geimer (1982), Hsu (1987), Liu and McNatt (1991), Xu and Winistorfer (1995), and Wu and Suchsland (1997).

In-plane swelling, known as linear expansion (LE), can be a very significant factor affecting the state of stress that exists in the material in both structural and nonstructural uses.

<sup>†</sup> Member of SWST.

<sup>1</sup> This paper (No: 00-22-0688) is published with the approval of the Director of the Louisiana Agricultural Experiment Station.

The differential swelling behavior of individual particles or flakes in wood composite panels can cause in-plane movements that result in high internal stresses. Thus, dimensional stability is also a major factor in the matter of durability, since the ultimate failure of an adhesive bond depends in part on these related stresses (Bryan 1962). Where OSB has been used as an exterior structural material, numerous instances of the so-called "window pane" phenomenon in roof applications have been attributed to the disregard of installation clearance between panels (Xu and Suchsland 1997). There are many factors that affect dimensional changes of a three-layer OSB board. Therefore, a theoretical study should be able to assess the importance of the significance of various factors.

In an earlier study (Wu 1999), the effects of panel processing variables on the in-plane stability behavior of single-layer oriented strand panels were investigated. It was shown that the shape of the LE-moisture content (MC) change curve varied with flake alignment level (FAL) and material direction (MD). The variation was attributed to the difference in the controlling mechanism for LE in various panels. Total LE from the oven-dry to water-soak condition, modulus of elasticity (MOE), and modulus of rupture (MOR) varied significantly with flake orientation distribution and density. LE, MOE, and MOR were correlated with the concentration parameter, density, resin content (RC), and MC using a power form equation. The experimental data form a database of layer properties for modeling three-layer, cross-laminated OSB. The current investigation dealt with three-layer boards fabricated under hot pressing. The objectives of the study were

- a) To investigate effects of panel processing variables on LE, MOE, and MOR of three-layer OSB with density gradient;
- b) To develop an analytical model for predicting LE, effective modulus (EM), and internal swelling stresses; and
- c) To verify the model by testing three-layer boards of different construction.

## BACKGROUND

### *In-plane stability of wood composites*

Several experimental studies have been conducted to investigate in-plane stability of wood composites. Zylkowski (1986, 1989) carried out comprehensive studies on the dimensional stability of structural panels including plywood, waferboard, and OSB. LE and TS of the panels tested were evaluated. The measured swelling data were expressed as the percentage of the total dimensional change from the oven-dry to water-soaked condition for a given humidity exposure. Results indicated that the relative LE was nearly constant for all materials and depended upon the panel MC. The major part of the expansion occurred at the low MC regions.

Using the LE rate, Suchsland and Xu (1991) classified wood composites into two main categories. The first category, including medium density fiberboard (MDF), has a swelling rate that approaches zero at the fiber saturation point (FSP). They called such panels substantially wood-like stable material since the swelling is due mainly to the swelling of the wood cell wall. The second category, including particleboard, has a swelling rate that gradually increases as the materials approach the FSP. They called such panels substantially unstable material since factors other than the swelling of the wood cell wall contributed to the swelling. One of the factors must be the partial breakdown of adhesive bonds resulting from excessive TS associated with horizontal density variation. This behavior reflects irreversibility of the swelling and of other associated properties.

The longitudinal free hygroscopic expansion coefficients and elastic recovery after constrained in-plane swelling were experimentally determined by Lang and Loferski (1995) for commercial plywood and OSB. Their results showed that the measured expansions were equal or larger for OSB as compared with those of plywood. Approximately 20 percent of the total hygroscopic expansion can be considered as elastic deformation for both

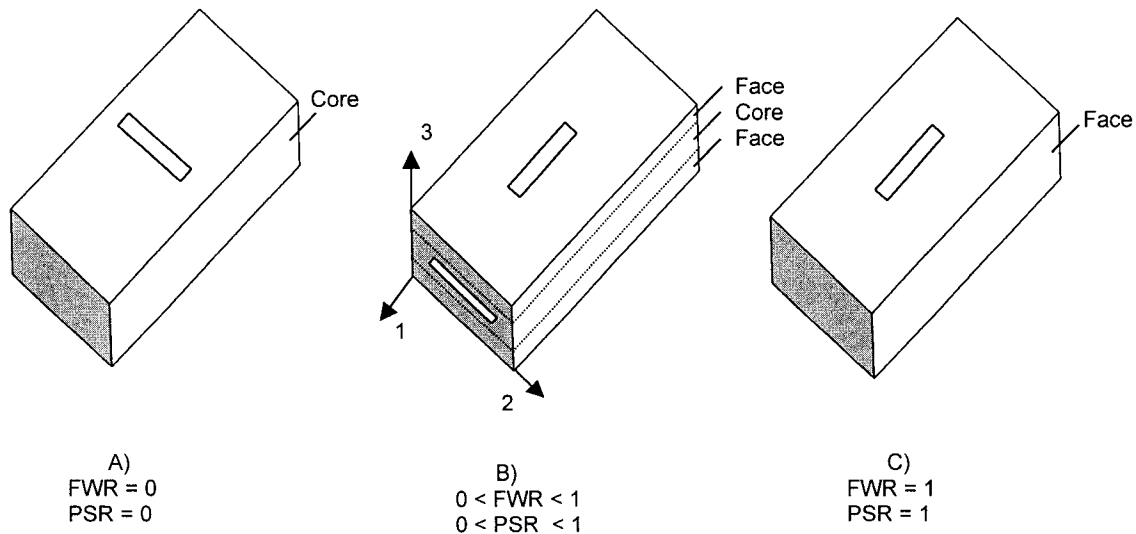


FIG. 1. A schematic of layered structure in OSB showing both single- (a and c) and three-layer (b) panels and three principal material directions (i.e., 1—parallel direction, 2—perpendicular direction, and 3—thickness direction). The rectangles on the graph show the orientation of wood flakes within each board type.

panel types. Wu and Suchsland (1996) measured LE along the two principal directions at different RH levels for five types of commercial OSB. They found that LE changed within the hygroscopic range as MC increased in the board. Despite differences in wood species and manufacturing variables, the broad features of LE were similar among various OSB products used. At lower MC levels, LE for all panels occurred at a greater rate and followed the longitudinal swelling behavior of solid wood. At higher MC levels, LE developed at a reduced rate and was due mainly to the effect of transverse swelling of wood. Improvement of FAL and better selection of other panel design variables would reduce this transverse effect and the overall LE of the panel.

When MC of wood composites changes, individual wood components within a panel become stressed as a result of the difference between actual dimensional change in the board and potential change of the particles or flakes. Thus, research efforts to improve the stability and durability of wood composites could be enhanced by basic information concerning interactions between individual particles or

flakes and the effect of these interactions on dimensional stability and internal stresses.

#### *Swelling stresses and strains in OSB*

OSB is manufactured in a layered structure by depositing different amounts of wood flakes (based on weight) in the face and core layers, respectively (Fig. 1). In a given panel, there are three principal directions (i.e., 1—parallel or machine direction, 2—perpendicular or cross-machine direction, and 3—thickness direction). Flake weight ratio (FWR), defined as a ratio of face layer flake weight to total panel flake weight, is normally used to describe the layered structure. When  $\text{FWR} = 0$  (Fig. 1a), all flakes are aligned along the perpendicular direction (i.e., single-layer boards—core). When  $0 < \text{FWR} < 1$  (Fig. 1b), part of the flakes are aligned in the parallel direction and part are in the perpendicular direction (i.e., three-layer boards). When  $\text{FWR} = 1$  (Fig. 1c), all flakes are aligned along the parallel direction (i.e., single-layer boards—face). For modeling purpose, panel shelling ratio (PSR), defined as a ratio of face layer thickness to total panel thickness, is more use-

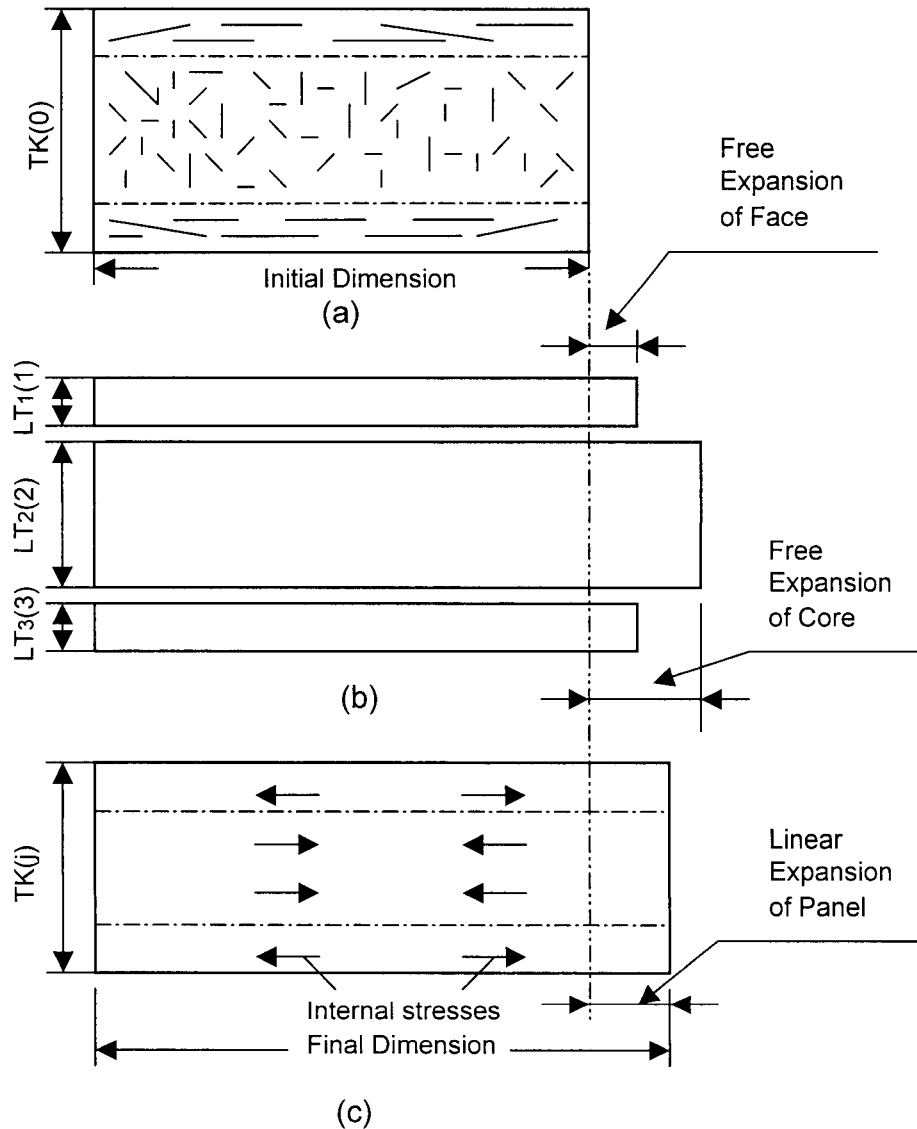


FIG. 2. A schematic of in-plane movement of OSB under swelling conditions. (a) initial panel dimension, (b) layer free expansion, and (c) final panel dimension with restricted layer expansion.

ful. Since the thickness for both face and core layers depends on the amount of wood flakes placed and the degree of compression during manufacturing, PSR varies with FWR and pressing variables.

A two-dimensional schematic of a three-layer OSB with varying flake orientation between face and core is shown in Fig. 2a. When panel MC is increased, there is a tendency for

each layer to expand, and if they were free to do so, they would expand freely to the layer dimension shown in Fig. 2b (free expansion). However, individual layers, as parts of a rigid unit, must elongate or shrink together to a final dimension (Fig. 2c). This creates internal stresses across the panel's thickness. Under the stresses, individual layers within the panel deform. The net deformation is the sum of two

main components: elastic-plastic (instantaneous) strain and free expansion strain. It should be pointed out that creep and mechano-sorptive strain also develop under the action of sustained swelling stresses (Wu and Milota 1995). However, for the simplicity of the analysis, these two strain components were ignored in this study (Talbot et al. 1979).

*Elastic-plastic strain* is produced immediately after the stress is created. Initially there is an elastic deformation that is proportional to the stress through an elastic modulus. This is followed by a plastic deformation that depends on the magnitude of the stress and MC level. Laufenburg (1983) characterized the stress-strain response of flakeboards to failure using the Ramberg-Osgood equation:

$$\epsilon_{EP} = \frac{\sigma}{E} + k \left[ \frac{\sigma}{E} \right]^n \quad (1)$$

where

$\epsilon_{EP}$  = stress-induced instantaneous strain (mm/mm);  
 $\sigma$  = stress (MPa);  
 $E$  = Young's modulus (MPa); and  
 $k, n$  = material constants.

As shown, three parameters (i.e.,  $E$ ,  $k$ , and  $n$ ) define the nonlinear stress and strain relationship for a given board type. Among the three variables,  $E$  varied with panel processing variables including density, FAL, RC, and panel MC (Geimer 1982; Wu 1999; Wu and Suchsland 1997). The model parameters ( $k$  and  $n$ ) were derived for flakeboard of various density and alignment levels at a given MC level by Laufenburg (1983). It is noticed that panel MC change significantly alters the stress-strain relationship for a given board. This effect can be accounted for by correcting the modulus for the given MC changes using E-MC relationships for OSB.

*Free expansion strain* is the dimensional change of an individual layer due to the moisture increase in absence of restraint. For solid wood, this is the inherent moisture-related wood swelling. For OSB, this is equivalent to the swelling of a thin flake layer with varying

flake orientation and density across panel thickness, similar to veneers in a sheet of plywood. Bryan (1962) and Xu and Suchsland (1997) developed analytical models based on elasticity to predict linear expansion of a flake layer with uniform density, considering variation in wood properties and flake orientation distribution. Experimental data on LE of oriented flake layers were developed by Geimer (1982) for Douglas-fir and by Wu (1999) for aspen. Nonlinear regression equations were developed to relate LE data to panel processing variables in those studies.

*Published work on modeling in-plane swelling of wood composites*

Several approaches have been developed to predict the in-plane linear dimensional properties of a three-layer wood composite board. Talbot et al. (1979) modeled linear expansion of three-layer Com\_PLY laminates. They demonstrated that internal stresses produced by the constrained hygroscopic expansion during moisture sorption are of significant magnitude. These stresses cause instantaneously plastic deformation in the material. Thus, an elastic analysis would lead to a significant overestimate of swelling stresses and underestimate in panel deformation. Tang et al. (1982) developed a three-dimensional model based on elasticity to predict the linear expansion of wood composites. Geimer (1982) considered vertical density gradient in predicting LE of a three-layer flakeboard. By using experimental data from single-layer boards of various densities and the measured density gradient of a three-layer flakeboard, the prediction was made by summing the values for each layer weighted for layer thickness. The approach, however, did not consider the interaction between layers of different densities. Lang and Loferski (1995) recognized the importance of the inelastic behavior of wood composites and determined the elastic expansion coefficients as the input to his model. Their approach, however, of treating a three-layer OSB as a uniform density panel and deriving the layer

property by a simple rule of mixture (based on layer thickness) did not represent boards with a vertical density gradient.

MODEL DEVELOPMENT

Predicting linear expansion and swelling stresses

The model considers a three-layer OSB board as a multi-layer laminate with varying flake orientation between face and core and layer density from panel surface to panel center (Figs. 2 and 3). Under the swelling condition, internal stress and strain develop due to the variation of layer swelling potentials. Superimposing the components of the stress-induced deformation on the free expansion results in LE of the panel. It is assumed that over a given MC change,  $\delta M$ , the LE strain increment for a flake layer is the sum of the increments of the elastic-plastic (i.e.,  $\epsilon_{EP}$ ) and free expansion strains (i.e.,  $\epsilon_{FE}$ ):

$$\delta\epsilon_{LE}(i, j) = \delta\epsilon_{EP}(i, j) + \delta\epsilon_{FE}(i, j) \quad (2)$$

where  $i$  is the sub-layer index in the board thickness direction and  $j$  is the step index in the RH/MC level (Fig. 3).

Among the strain components, the elastic-plastic strain increment is related to the stress increment as:

$$\delta\epsilon_{EP}(i, j) = D_{EP}(i, j) \delta\sigma(i, j) \quad (3)$$

where  $D_{EP}$  is the elastic-plastic compliance, which varies with both position and MC level for OSB. The compliance is defined through Eq. (1) as:

$$D_{EP}(i, j) = \frac{1}{E(i, j)} \left[ 1 + k(i, j)n(i, j) \left( \frac{\sigma(i, j)}{E(i, j)} \right)^{n(i, j)-1} \right] \quad (4)$$

Equation (4) transfers the nonlinear stress-strain relationship (Eq. 1) into a piecewise linear stress-strain relation, in which the local compliance varies with local stress and MC. Among the model parameters, Laufenberg (1983) developed values of  $k$  and  $n$  for single-

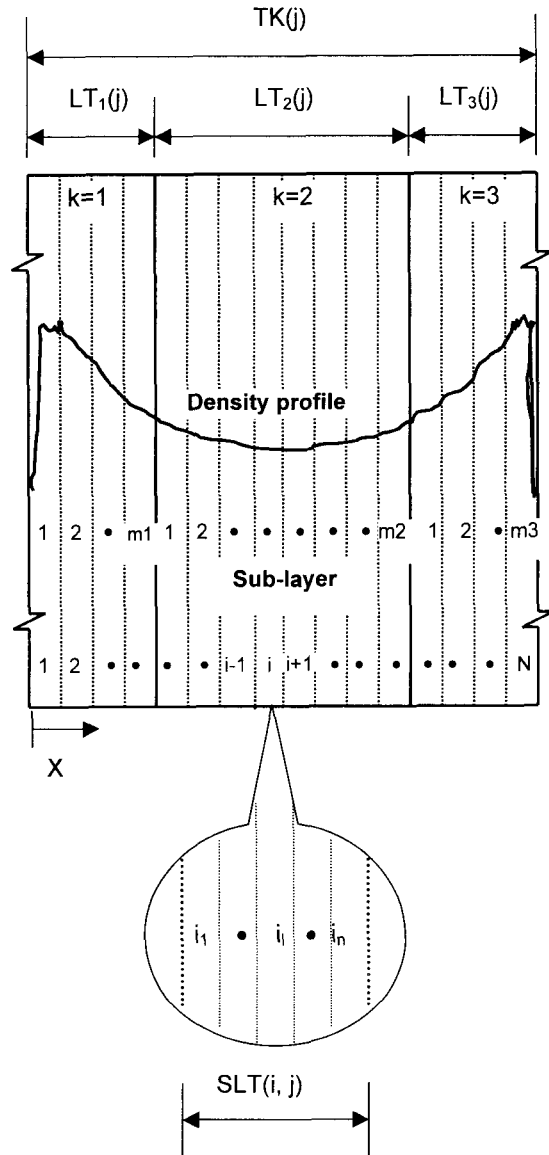


FIG. 3. A schematic of subdividing panel thickness and density profile for modeling purpose. Variables shown are:  $i$ —index for sub-layer,  $j$ —index for RH step,  $k$ —index for layer,  $l$ —index for density points in a sub-layer,  $LT$ —layer thickness,  $m$ —total number of sub-layers in a given layer,  $n$ —total number of density points in a sub-layer,  $N$ —total number of sub-layers in the panel,  $SLT$ —sub-layer thickness, and  $TK$ —panel thickness.

layer OSB under both tension and compression loadings. The regression models relating E to panel processing variables in both parallel and perpendicular directions were developed by Wu (1999). The elastic modulus, E, as a function of MC, for OSB was developed by Wu and Suchsland (1997). Combining these relationships (Table 1) allows defining the stress-strain curve under various processing and MC conditions.

The free expansion strain increment is obtained as:

$$\delta\epsilon_{FE}(i, j) = \left[ \frac{dF(i, j)}{dM(i, j)} \right] \delta M(i, j) \quad (5)$$

where the function F represents the nonlinear regression function relating free expansion strain to panel processing variables and MC change (Table 1: Free Linear Expansion, Wu 1999). Substituting Eqs. (3), (4), and (5) into Eq. (2) and solving for the stress increment, one obtains:

$$\delta\sigma(i, j) = \left[ \frac{\delta\epsilon_{LE}(i, j) - \delta\epsilon_{FE}(i, j)}{D_{EP}(i, j)} \right] \quad (6)$$

Subject to the equilibrium (i.e., net force across board thickness is equal to zero) and compatibility conditions (i.e., all sub-layers reach the same final dimension), the LE strain increment is:

$$\delta\epsilon_{LE}(j) = \frac{\int_0^{TK(j)} \left[ \frac{\delta\epsilon_{FE}(i, j)}{D_{EP}(i, j)} dx \right]}{\int_0^{TK(j)} \left[ \frac{1}{D_{EP}(i, j)} dx \right]} \quad (7)$$

where TK(j) is the panel thickness (mm) and x is the coordinate across board thickness. It is noticed that the thickness of individual layers increases with an increase in MC due to TS. The increase in layer thickness over a given MC change can be calculated using the thickness swelling rate (TSR) data for OSB (Ren 2000). Equations (6) and (7) allow the determination of the internal stresses and panel LE, provided that various strain components are known. The same procedure applies to

TABLE 1. Summary of material properties for model input.<sup>1,2</sup>

Material properties	Material direction	
	Parallel	Perpendicular
<b>Stress-strain Curve<sup>a</sup></b>		
Tension	$\epsilon_{EP} = \sigma/E + 4.58 \times 10^{11} [\sigma/E]^{5.93}$	$\epsilon_{EP} = \sigma/E + 4.79 \times 10^7 [\sigma/E]^{4.37}$
Compression	$\epsilon/EP = \sigma/E + 1.76 \times 10^9 [\sigma/E]^{5.46}$	$\epsilon/EP = \sigma/E + 4.43 \times 10^7 [\sigma/E]^{4.71}$
Elastic Modulus <sup>b</sup>	$E = 12.1314 SG^{1.1589} \kappa^{0.1411}$	$E = 3.6324 SG^{1.1544} \kappa^{-0.2842}$
Elastic Modulus-MC Relationship <sup>c</sup>	$E(M) = E(M_0) [1 - 0.0316 (M - M_0)]$	$E(M) = E(M_0) [1 - 0.0355 (M - M_0)]$
Linear Expansion <sup>d</sup>	$LE = 0.02837 RC^{-0.1877} SG^{-0.7706} \kappa^{-0.1616} (M - 3)^{0.589}$	$LE = 0.05 FC^{0.4839} SG^{0.6285} \kappa^{0.3281} (M - 3)^{0.7215}$
Parameters in EMC-RH Model <sup>e</sup>	$M_v = 21.4388 RC^{0.0501} SG^{-0.2780} \kappa^{0.0044}$ $A = 4.93 RC^{-0.0499} SG^{0.1464} \kappa^{-0.005}$ $TSR = 0.0827 RC^{-0.2727} SG^{0.3664} \kappa^{-0.0234} M^{1.1592}$	
<b>Thickness Swelling Rate (TSR)<sup>f</sup></b>		

<sup>1</sup> Data Source: <sup>a</sup> Laufenberg (1983)—6% moisture content, <sup>b</sup> Wu (1999)—6% moisture content, <sup>c</sup> Wu and Suchsland (1998)—Commercial OSB, <sup>d</sup> Wu (1999)—MC change for LE from the 3% level, <sup>e</sup> Wu and Ren (2000), and <sup>f</sup> Ren (2000).  
<sup>2</sup> Variables shown are:  $\epsilon_{ij}$ —Elastic/plastic strain (mm/mm),  $\sigma$ —stress (MPa), E—Young's modulus (MPa), SG—specific gravity,  $\kappa$ —concentration parameter, M—moisture content (%),  $M_0$ —reference moisture content (%), RC—resin content (%), LE—linear expansion (%), and TSR—thickness swelling rate (%TS/%MC).

both directions parallel and perpendicular to the major alignment direction of the face flakes.

#### Predicting effective modulus

Panel effective modulus, EM, is calculated using the equation derived by Bodig and Jayne (1993) based on the laminate bending theory. The equation has the form:

$$EM(j) = \frac{1}{I(j)} \sum_{i=1}^N E(i, j) \times \{I_0(i, j) + CSA(i, j)[d(i, j)]^2\} \quad (8)$$

where EM(j) is the effective modulus of OSB at the jth RH/MC step, I(j) is the moment of inertia of the entire OSB panel, E(i, j) is the MOE of the ith sub-layer,  $I_0(i, j)$  is moment of inertia of the ith sub-layer, CSA(i, j) is cross-sectional area of the ith sub-layer, d(i, j) is the distance between the ith layer center line and the centroidal plane of the panel, and N is the total number of sub-layers across panel thickness.

#### COMPUTER IMPLEMENTATION

A computer program was written using Fortran PowerStation to implement the algorithm outlined above. For a given board type along a given material direction (i.e., parallel or perpendicular), the calculation proceeds as follows.

1. FWR loop begins. Panel thickness corresponding to the initial given RH condition, TK(j = 0), is divided into three parts to represent face (k = 1), core (k = 2), and face (k = 3) layer, respectively (Fig. 2). The layer thickness,  $LT_k(j)$ , is determined according to

$$\begin{aligned} \text{Face } LT_1(j) \text{ or } LT_3(j) &= \left[ \frac{1}{2}TK(j) \right] \prod \\ \text{Core } LT_2(j) &= TK(j) \\ &- [LT_1(j) + LT_3(j)] \end{aligned} \quad (9)$$

where the function  $\Pi$  is the relationship between panel FWR and PSR.

2. The face and core layers are further divided into a number of m(k = 1, 2, 3) sub-layers, giving a total of N sub-layers across the panel thickness. Note that m(k) may differ from face to core layers. Each sub-layer has a thickness of SLT(i, j) as shown in Fig. 3.
3. The mean density,  $\rho(i, j)$ , for each sub-layer is evaluated according to measured density profile and number of density points within the sub-layer using numerical integration techniques.
4. EMC of each sub-layer corresponding to the given initial RH level (j = 0) is calculated using Nelson's sorption model (Wu and Ren 2000):

$$\begin{aligned} EMC(i, j) &= M_v(i, j) \left\{ 1.0 - \frac{1}{A(i, j)} \right. \\ &\quad \left. \times \text{Ln}[(-33.1125)\text{Ln}[RH(j)]] \right\} \end{aligned} \quad (10)$$

where the model parameters,  $M_v(i, j)$  and  $A(i, j)$ , as functions of panel processing variables are determined using the relationship listed in Table 1 (Wu and Ren 2000) and the calculated density for each sub-layer (step 3).

5. E(i, j) for each sub-layer is calculated based on the layer properties using the relationship developed by Wu (1999) (Table 1: elastic modulus). The panel EM is evaluated using Eq. (8) considering the relative position of each layer.
6. RH loop begins. RH increases by a  $\Delta RH$  (e.g., 5%). The sub-layer EMC(i, j) is recalculated using Eq. (10) and the new RH value. The new sub-layer thickness is calculated as

$$\begin{aligned} SLT(i, j) &= SLT(i, j - 1) \\ &\quad \times [1 + TSR(i, j)\Delta EMC(i, j)] \end{aligned} \quad (11)$$

where TSR(i, j) is the layer TS rate in

- %TS/%MC. TSR as a function of processing variables (Table 1) is taken from Ren (2000). The new sub-layer density,  $\rho(i, j)$ , is evaluated after accounting for the layer TS.
7. The sub-layer  $E(i, j)$  is corrected for changes in density and EMC using E-processing variables (Wu 1999) and E-MC (Wu and Suchsland 1997) relationships shown in Table 1. The mean modulus over the given MC change step is calculated as  $[E(i, j) + E(i, j - 1)]/2$ .
  8. The compliance defined in Eq. (4),  $D_{EP}(i, j)$ , is calculated using the mean modulus value (step 7), parameters  $k$  and  $n$  defined in Table 1 (Laufenberg 1983), and the stress value for the layer. Note that the values of  $k$  and  $n$  depend on whether the layer is under tension or compression as specified in Table 1.
  9. The sub-layer strain increments,  $\delta\epsilon_{EP}(j)$  and  $\delta\epsilon_{FE}(j)$ , due to increase in layer MC are calculated using Eqs. (3) and (5), respectively.
  10. Increments in panel strain,  $\delta\epsilon_{LE}(j)$ , and internal stresses,  $\delta\sigma(i, j)$ , are calculated using equilibrium and compatibility conditions (Eqs. 7 and 6). The control is shifted back to step 6 (RH change) and the calculation is repeated.
  11. FWR is updated. The control is shifted back to step 1 (FWR change) and the calculation is repeated.

#### EXPERIMENTAL

The experimental procedures were given in detail in an earlier paper (Wu 1999) and are reviewed here in brief. Discussion is further directed towards the three-layer, cross-laminated boards, which are of particular relevance in this report.

Thirty-two three-layer OSB panels were manufactured using 76-mm-long, disc-cut aspen flakes. There were two RC levels (4% and 6%), two FALs (high and low), four FWRs (0.3, 0.4, 0.5, and 0.6), one target density (specific gravity = 0.70), one wax level (0.5%),

and two replications. Eight single-layer boards (two resin levels, two alignment levels, and two replications) were also made to simulate panels at a FWR of 0 or 1. All boards were manufactured with a 10% mat MC before pressing and were pressed in a conventional manner for 8 min at a temperature of 190°C. Flake alignment distribution for each panel was determined by measuring randomly selected 120 flakes from the top surface of each panel and by fitting the measured flake angles to the von Mises distribution (Wu 1999).

Three 50.4 × 50.4 × 12.5-mm specimens were cut from each panel to determine layer thickness and density profile across panel thickness. Two parallel lines were drawn on each of the four edges for each sample under microscope to separate the two face layers from the core. All samples were conditioned to reach equilibrium at 45% (dry condition) and then at 93% (wet condition) RH levels. Layer thickness was measured with a digital caliper (0.01-mm accuracy) using lines drawn on each edge. Measurements from all four edges were averaged. Measured layer thickness and total panel thickness were used to calculate actual panel shelling ratios, PSR, for each given FWR. A linear regression analysis was done to establish a quantitative relationship between PSR and FWR. The density profile in the specimen thickness direction was determined on a Quintek Density Profiler (Model QDP-01X). The specimens were positioned during measurements with the top surface as the starting position. Discrete density values for 0.0508-mm thickness increments were obtained from the measured density profiles. The density values at the same position for the six specimens from each panel type were averaged to obtain the average density profile for each panel.

Two samples, 38.1 × 304.8 × 12.7 mm, were cut along each of the two principal directions from each board for LE tests. They were labeled according to board type, orientation (parallel or perpendicular), and replication number. Two holes (1.1 mm in diameter) 254 mm apart were drilled along the long di-

mension of each specimen and a small rivet (1.0 mm in diameter), dipped in epoxy glue, was plugged into each of the two holes. After the glue had set, crossed hairlines were carefully cut on the tip of each rivet using a sharp razor blade. The hairlines facilitated LE measurements with an optical comparator. All specimens were initially dried in a convection oven at 60°C to reach a constant weight. Measurements including specimen weight, length, width, thickness, reference dimension between the two rivets, and layer thickness of each specimen were made in the dry state. All specimens were conditioned in a computer-controlled conditioning chamber according to: Dry state  $\Rightarrow$  35%  $\Rightarrow$  55%  $\Rightarrow$  75%  $\Rightarrow$  85%  $\Rightarrow$  93% RH. Finally, all specimens were oven-dried for 24 hours. The measurements were repeated after reaching equilibrium at each specified RH level and at the oven-dry condition.

Static bending specimens,  $76.2 \times 355.6 \times 12.7$  mm, were cut along the two principal directions of each panel according to ASTM D1037-96 (ASTM 1996). One parallel and one perpendicular specimen from each panel were prepared, totaling 40 specimens for each direction. This gave two replications for each combination of density, alignment level, and RC. The specimens were conditioned to equilibrium at 45% RH and 25°C. Their weight and size (i.e., length, width, and thickness) were measured before testing. Bending tests were made on a Model 4260 INSTRON machine with a computer-controlled data acquisition system. After the test, each specimen was weighed and oven-dried to determine its MC on the OD basis. Statistical comparisons of the data were made to show the effects of various processing variables on measured MOE, MOR, and LE along the two principal directions. To eliminate the effect of sample density variation on measured MOE and MOR, specific MOE (MOE/SG) and specific MOR (MOR/SG) were used in the analysis.

#### RESULTS AND DISCUSSION

Experimental data on panel processing variables, static bending, and in-plane swelling

properties of the OSB along the two principal directions are summarized in Table 2. The boards at high and low alignment levels had mean concentration parameters (Wu 1999) of 6.23 and 1.87, respectively. The corresponding percentages of alignment (Geimer 1982) were 78 and 50. The overall mean panel specific gravity was 0.70. All panels had vertical density gradient across panel thickness as shown in Wu and Ren (2000).

#### *Effect of processing variables on measured MOE, MOR, and LE*

*Flake alignment level.*—The effect of FAL on specific MOE, specific MOR, and LE was significant at the 5% significance level (Table 3). For panels with FWR = 0 or 1 (i.e., single-layer boards), change in the alignment level led to significant change in MOE, MOR, and LE values (Table 2). At FWR = 0, panel MOE and MOR increased and LE decreased in the parallel direction, while MOE and MOR decreased and LE increased in the perpendicular direction as the alignment level increased. The opposite was true for panels with FWR = 1. For three-layer boards ( $0 < \text{FWR} < 1$ ), the effects of FAL on both bending and swelling properties were more complicated as FWR also affected their values. At the 6% RC, FAL had significant effect on MOE at the 5% significance level. There was, however, no significant effect of FAL on MOE at the 4% RC level. Thus the combined effect of RC and FAL was not significant (Table 3). At a given FWR and RC level, panels at the high FAL had smaller LE, and thus had improved in-plane dimensional stability, compared with the panels at the lower FAL (Table 2).

*Flake weight ratio.*—MOE, MOR, and LE of the OSB panels varied largely with FWR at a given alignment and RC level as shown in Table 2. As FWR increased, both MOE and MOR increased in the parallel direction and decreased in the perpendicular direction. On the other hand, LE decreased in the parallel direction and increased in the perpendicular direction as FWR increased. Statistical analy-

TABLE 2. Summary of test results of static bending and LE properties along the two principal directions.

Board type <sup>a</sup>	FWR	K <sup>b</sup>	Parallel					Perpendicular				
			MC <sup>c</sup> (%)	SG <sup>c</sup>	MOE <sup>c</sup> (MPa)	MOR <sup>c</sup> (MPa)	LE <sup>d</sup> (%)	MC <sup>c</sup> (%)	SG <sup>c</sup>	MOE <sup>c</sup> (MPa)	MOR <sup>c</sup> (MPa)	LE <sup>d</sup> (%)
HAL	0.0	6.71	4.5	0.71	1459.8	12.43	1.74	4.3	0.73	14849.7	93.00	0.07
4% RC	0.3	6.35	4.6	0.68	8062.5	46.36	0.17	4.6	0.67	6779.9	53.87	0.12
	0.4	5.02	4.7	0.73	9231.1	59.83	0.12	4.6	0.68	5130.2	42.97	0.15
	0.5	6.57	4.6	0.68	12009.4	78.53	0.11	4.4	0.72	4955.8	44.68	0.14
	0.6	6.63	4.6	0.67	11516.4	65.60	0.11	4.5	0.68	2957.9	30.14	0.22
	1.0	6.71	4.3	0.73	14849.7	93.00	0.07	4.5	0.71	1459.8	12.43	1.74
HAL	0.0	5.82	4.6	0.71	1495.3	14.55	1.65	4.3	0.74	15621.8	94.31	0.06
6% RC	0.3	5.78	4.5	0.68	8720.9	54.55	0.15	4.3	0.75	7507.6	63.59	0.11
	0.4	6.09	4.6	0.65	9689.5	59.22	0.13	4.5	0.69	5909.5	51.27	0.15
	0.5	6.45	4.5	0.68	11023.5	70.79	0.11	4.4	0.70	3503.9	37.02	0.16
	0.6	6.99	4.5	0.69	12157.6	70.04	0.10	4.3	0.65	2528.4	24.75	0.18
	1.0	5.82	4.3	0.74	15621.8	94.31	0.06	4.6	0.71	1499.3	14.55	1.65
LAL	0.0	2.42	4.8	0.67	2836.2	22.58	0.52	4.8	0.63	8707.1	57.17	0.08
4% RC	0.3	1.54	4.5	0.73	7597.2	53.92	0.20	4.4	0.72	6812.3	56.24	0.15
	0.4	1.51	4.6	0.73	9310.4	62.92	0.15	4.5	0.72	5503.8	47.22	0.16
	0.5	1.84	4.6	0.72	9675.7	61.22	0.14	4.5	0.72	5252.5	47.65	0.16
	0.6	1.32	4.7	0.66	8262.5	51.63	0.11	4.5	0.70	4132.3	35.78	0.24
	1.0	2.42	4.8	0.63	8707.1	57.17	0.08	4.8	0.67	2836.2	22.58	0.52
LAL	0.0	2.46	4.5	0.75	2876.9	26.57	0.56	4.8	0.68	11685.3	81.35	0.09
6% RC	0.3	1.47	4.6	0.66	6811.3	42.35	0.18	4.3	0.70	6548.9	52.53	0.16
	0.4	1.67	4.5	0.69	7835.1	54.78	0.18	4.4	0.71	5271.8	43.05	0.18
	0.5	1.79	4.5	0.67	8372.8	53.95	0.14	4.6	0.66	3936.8	35.11	0.20
	0.6	1.62	4.6	0.68	9020.8	56.66	0.11	4.6	0.69	4680.3	37.73	0.23
	1.0	2.46	4.5	0.75	11685.3	81.35	0.08	4.8	0.68	2876.9	26.57	0.56

<sup>a</sup> HAL—High alignment level; LAL—Low alignment level; RC—Resin content.

<sup>b</sup> K—Concentration parameter (Wu 1999).

<sup>c</sup> The values shown are means of two samples at each condition.

<sup>d</sup> LE—Linear Expansion of OSB panels conditioned from 35% to 93% RH. The values shown are means of four samples at each condition.

TABLE 3. Results of the two factorial ANOVA on the effect of panel processing variables on LE, specific MOE, and specific MOR.

Variables <sup>a</sup>	LE (mm/mm)	Specific MOE <sup>b</sup> (MPa)	Specific MOR <sup>c</sup> (MPa)
AL	S <sup>d</sup>	S	S
FWR	S	S	S
MD	NS <sup>e</sup>	S	S
RC	NS	NS	NS
AL × FWR <sup>f</sup>	S	S	S
MD × FWR <sup>f</sup>	S	S	S
RC × FWR <sup>f</sup>	NS	NS	NS
RC × AL <sup>f</sup>	NS	NS	NS
MD × AL <sup>f</sup>	NS	NS	NS
RC × MD <sup>f</sup>	NS	NS	NS

<sup>a</sup> AL—alignment level, FWR—flake weight ratio, MD—material direction, and RC—resin content.

<sup>b</sup> Specific MOE = MOE/Specific gravity (SG).

<sup>c</sup> Specific MOR = MOR/Specific gravity (SG).

<sup>d</sup> S—significant at the 5% significance level.

<sup>e</sup> NS—not significant at the 5% significance level.

<sup>f</sup> Combined effect of the two variables shown.

sis (Table 3) shows that the effect of FWR was significant for LE and specific MOR and MOR at the 5% significance level. The combined effect of FWR with alignment level and material direction was also significant (Table 3). Therefore, FWR is one of the primary variables, which controls in-plane bending and swelling properties of OSB.

*Resin content.*—For a given panel type, measured MOE and MOR were slightly larger and LE was smaller at the 6% RC level, compared with the values at the 4% RC level. However, statistical analysis showed no significant effect of RC on specific MOE, specific MOR, and LE at the two RC levels used (Table 3). The combined effect of RC with FWR, material direction, and alignment level was also not significant. Thus, RC at the levels used was not a significant variable influencing

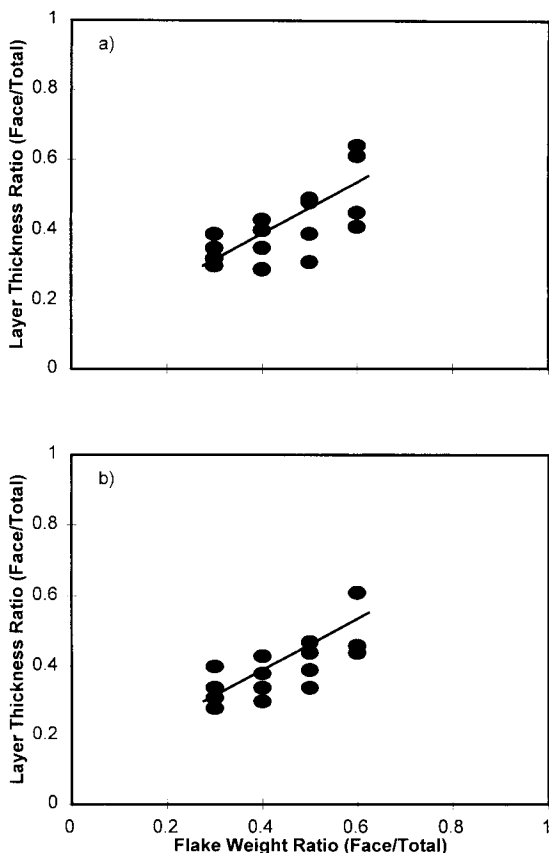


FIG. 4. Relationship between panel shelling ratio (PSR) and flake weight ratio (FWR) of OSB under a: dry (5.2% MC) and b: wet (21.6% MC) conditions. Symbols are measured data and lines are regression results.

the OSB's properties. The results agreed with earlier findings for the single-layer, uniform density oriented strand panels (Wu 1999).

*Material direction.*—There was significant effect of material direction (parallel or perpendicular) on measured specific MOE and MOR (Table 3). The effect of material direction on LE was significant for the single-layer boards (FWR = 0 and 1). For the three-layer boards (FWR = 0.3, 0.4, 0.5, and 0.6), however, the effect of material direction on LE was not significant mainly due to large variability of the LE data.

#### *Relationship between PSR and FWR*

Variation of the measured PSR in relation with FWR is shown in Fig. 4 (a: dry and b:

wet). Actual MC of the specimens at the dry and wet conditions averaged 5.2% and 21.6%, respectively. Measured layer thickness data showed a considerable variation at each FWR under both dry and wet conditions. The variation was due to the fact that there was no uniform and clear boundary between face and core layers for a given board structure. During pressing, flake layers within the plane of the panel were bent to various degrees depending on the actual number of flake layers at the given positions. This caused a wave-like boundary between face and core layers, which made it difficult to determine PSR accurately for a given panel.

Based on the measured data, the following relationships between PSR and FWR were established for the material:

Dry

$$\text{PSR} = \prod (\text{FWR}) = 0.1375 + 0.6125\text{FWR}$$

$$r^2 = 0.47$$

Wet

$$\text{PSR} = \prod (\text{FWR}) = 0.1208 + 0.6401\text{FWR}$$

$$r^2 = 0.66 \quad (12)$$

PSR would be directly proportional to FWR with proportionality equal to 1, if face and core layers were compressed to the same degree during hot pressing. However, due to densification of the face layers, the slope of the PSR-FWR line was smaller than unity. Thus, the slope of the PSR-FWR line for a given panel would depend on the degree of compression between face and core layers. The regression models for both dry and wet conditions showed similar trends. The larger slope of the PSR-FWR line under the wet condition indicated a larger TS rate of the face layer compared with the core layer during the wetting process. The regression equations were used in the model to determine layer thickness between face and core (Eq. 9) for a given board type.

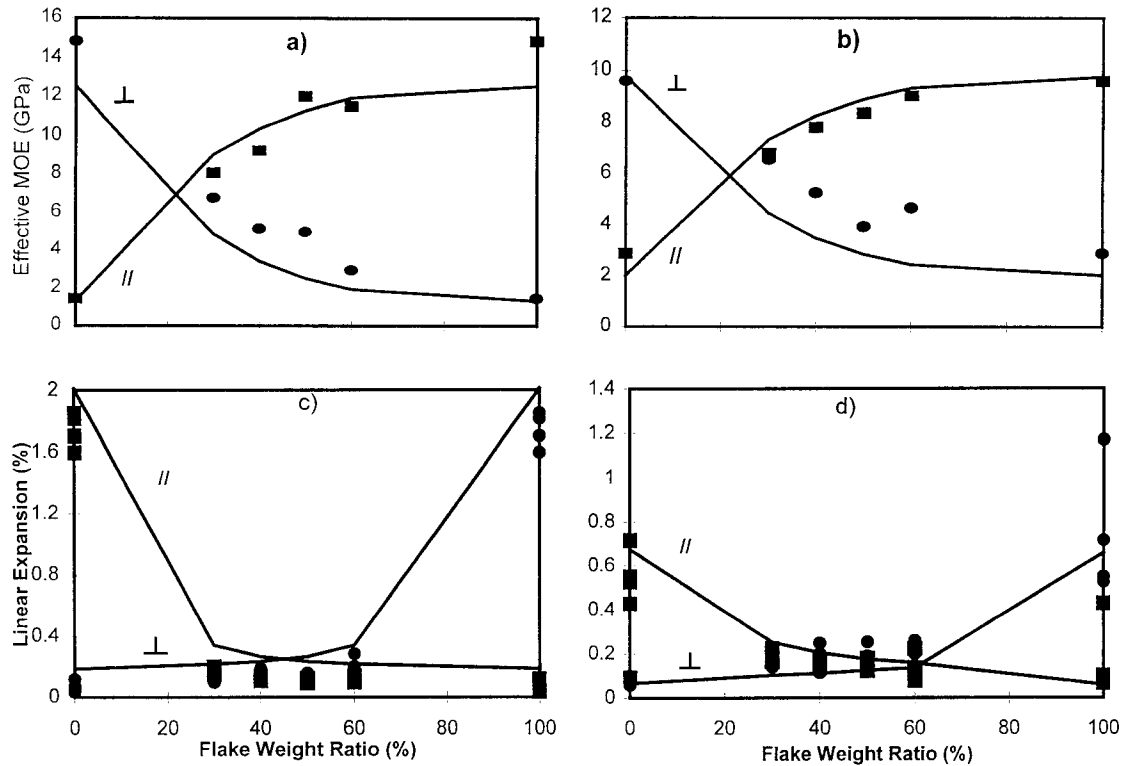


FIG. 6. Effective modulus (a and b) and linear expansion (c and d) as a function of panel FWR for panels at high FAL and 4% RC (a and c) and low FAL and 6% RC (b and d). Symbols are measured data and lines represent predicted values.

ing). The LE values along the two directions reached a similar value at FWR = 0.6. This point was shifted to the right compared with EM curves (Fig. 6a and Fig. 6b). After this point, LE in the parallel direction became smaller than the value in the perpendicular direction. The model's prediction of LE under all FWRs matched experimental data well, considering the complex nature of OSB's swelling behavior.

From the above discussion, it can be seen that the proposed model can be used to predict in-plane EM and LE of OSB accounting for various interactive factors such as FAL, FWR, density gradient, and RC. This provides an analytical tool for optimizing the balance between EM and LE in the manufacturing of OSB.

#### *Predicting swelling stress and strain*

Typical swelling stress distributions predicted by the model are shown in Fig. 7a for panels at a given FWR (i.e., 0.3) subjected to two RH exposure conditions (i.e., 35% to 45% and 35% to 93%) and Fig. 7b for panels at various FWRs (i.e., 0.3, 0.5, and 1) subjected to the same RH exposure condition (i.e., 35% to 93%). For a given panel type, the magnitude of the swelling stresses increased with an increase in the RH exposure range. Under the swelling condition shown in Fig. 7a, two face layers were subjected to tension and the core layer was subjected to compression for the parallel specimens. In these specimens, the face layers had flakes oriented along the parallel direction and the core had flakes oriented along the perpendicular direction. This led to

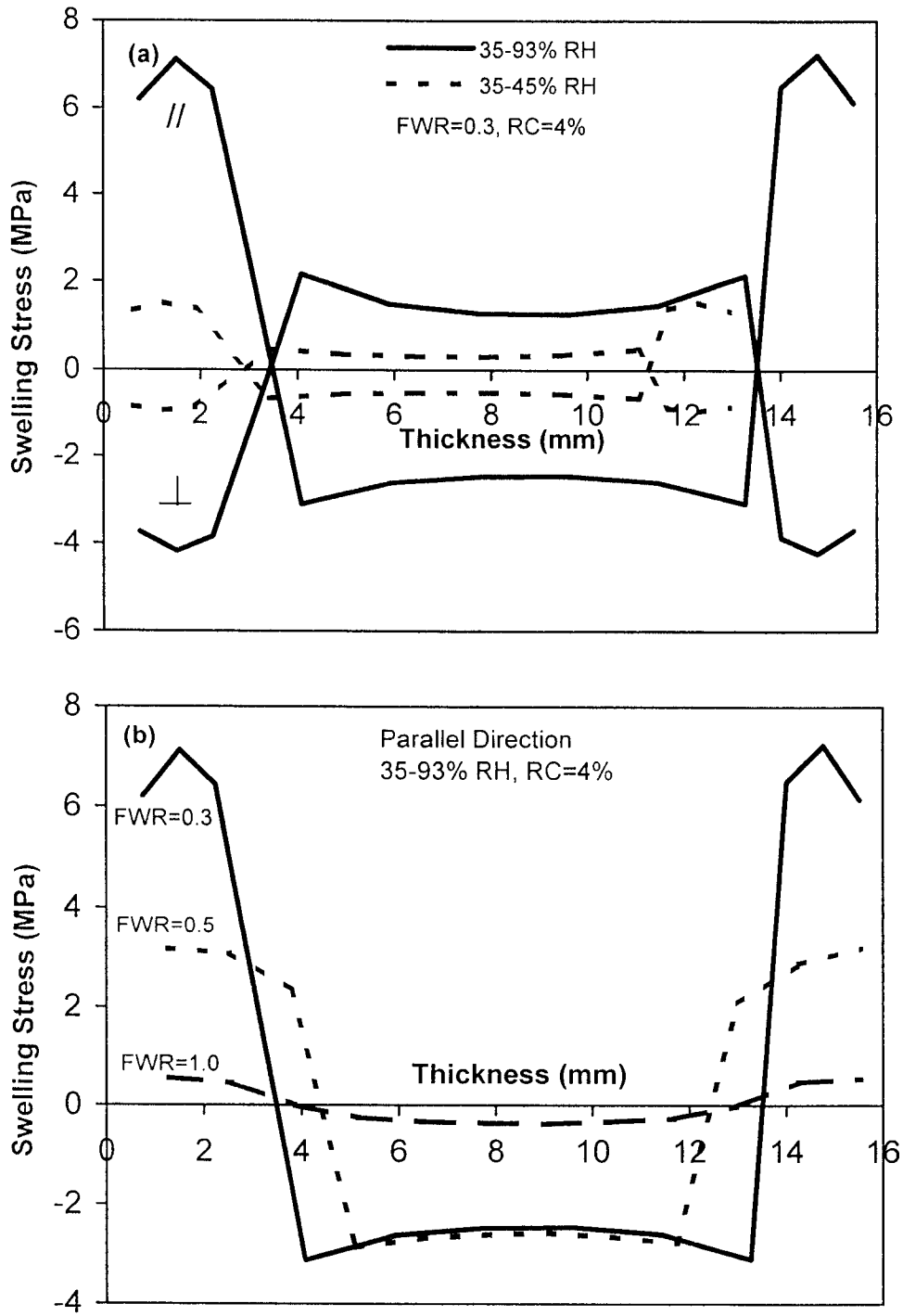


FIG. 7. Predicted internal swelling stresses across panel thickness. (a) panels of a given FWR (0.3) at two RH exposure levels and (b) panels of various FWRs at one RH exposure condition (35% to 93%RH).

### *Relationship between LE and MC change*

A curvilinear relationship between LE and MC change (MCC) was observed for the OSB (Fig. 5). Due to the asymptotic nature of the LE-MCC curve, LE rate was larger at the lower MC levels. As the MC levels increased, however, the swelling rate became smaller. The LE-MCC curves in the parallel direction showed more asymptotic tendencies than those in the perpendicular direction. For single-layer, oriented strand panels, Wu (1999) showed that the LE-MCC curve in the parallel direction was curvilinear. The curve was almost linear in the perpendicular direction, following the transverse swelling behavior of solid wood. The curvilinear behavior of LE observed in this study for the three-layer boards indicated the dominant effect of the flake layer along the parallel direction for controlling the LE behavior of OSB. For a given MCC, FWR increase led to LE decrease in the parallel direction and to LE increase in the perpendicular direction (Table 2 and Fig. 5). This indicated the balancing effect of the cross-lamination in OSB. Despite the difference in actual LE values for boards at various FWRs, the general shape of LE-MCC curves was similar among the boards of different constructions.

For a given MCC, the measured LE data varied significantly among the specimens tested, similar to the behavior observed in other studies (e.g., Wu and Suchsland 1996; Wu 1999). This was caused by the difference in actual flake orientation distribution among various specimens. The predicted LE as a function of MCC for boards at various FWRs matched the experimental data reasonably well, considering the complex nature of OSB itself and various empirical relationships for the material properties used.

### *Predicting effective modulus and LE as a function of FWR*

Predicted effective modulus, EM, of the OSB as a function of FWR is plotted in comparison with the experimental data in Fig. 6a and Fig. 6b for high and low alignment panels,

respectively. The effect of FWR on the magnitude of EM along the two different directions is clearly seen in the graph. At a given alignment level, EM increased in the parallel direction and decreased in the perpendicular direction as FWR increased (Fig. 6a and Fig. 6b). At the low FWR, EM in the machine (or parallel) direction was smaller than the value in the cross-machine (or perpendicular) direction. This was due to the fact that only a small portion of the flake was aligned in the parallel direction. As FWR increased, EM in the parallel direction increased due to an increased amount of flakes aligned in this direction. At the same time, EM in the perpendicular direction decreased due to the decreased amount of flakes aligned in the direction. EM in both directions reached a similar value at a FWR value between 0.2 and 0.3. Further increase in FWR led to a larger EM in the parallel direction compared to the value in the perpendicular direction. At a given FWR, no significant effect of RC on EM was observed at both alignment levels. However, EM was significantly influenced by flake alignment level as shown in the graph (Fig. 6a and Fig. 6b). At both alignment levels, predicted EM matched closely to the measured values at various FWRs. The general EM-FWR trend was also in close agreement with those reported for laboratory-made and commercial OSB (Xu 2000; Wu and Suchsland 1996).

Predicted LE curves as a function of FWR for the OSB are shown in Fig. 6c and Fig. 6d for high and low alignment panels, respectively. Similar to EM, FWR played a significant role in balancing the LE values between the two directions as shown in the graphs. However, the LE-FWR relationship at a given direction followed a reverse trend compared with EM. At  $FWR = 0$  (i.e., single-layer boards with all flakes aligned along the perpendicular direction), LE in the parallel direction was many times larger than the value in the perpendicular direction. The effect of alignment level on LE is clearly seen with these single-layer boards (Fig. 6c versus Fig. 6d). The decrease in the alignment level

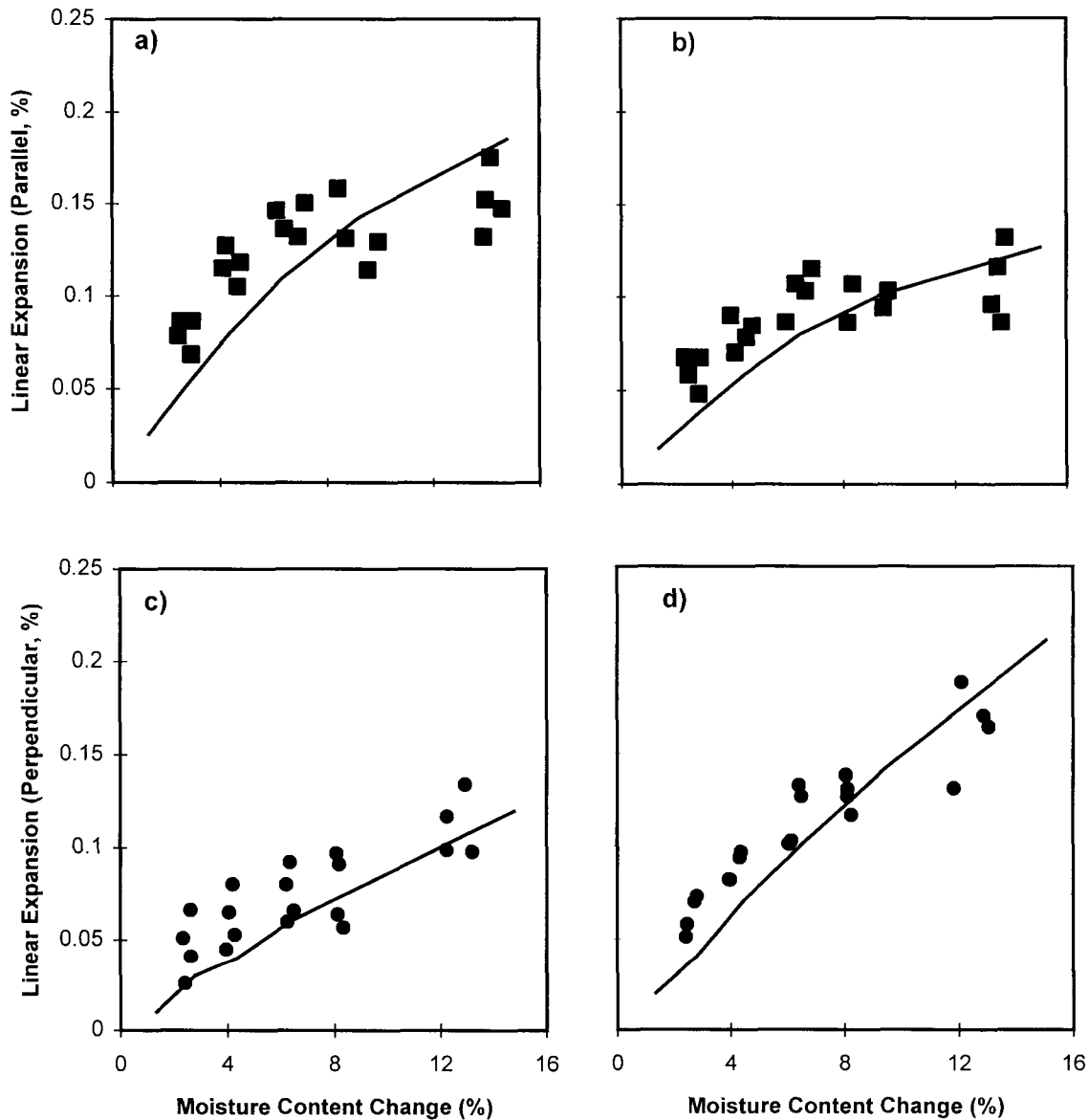


FIG. 5. Linear expansion as a function of sample MC change along the two principal directions (parallel: a and b; perpendicular: c and d) for the three-layer panels at two FWRs (0.3: a and c; 0.5: b and d). The starting MC was on average 5.2%. Data shown were from panels at low FAL and 6% RC. Symbols are measured data and lines represent predicted values.

caused significant LE decrease in the parallel direction, while there was relatively little change in the perpendicular direction. As the FWR increased, LE in the parallel direction decreased due to the contribution from the cross-laminated flakes in the face layer orient-

ed along the parallel direction (less longitudinal wood swelling). At the same time, LE in the perpendicular direction increased due to the contribution from the cross-laminated flakes in the face layer oriented along the parallel direction (more transverse wood swell-

a smaller free LE in the face layers and a larger free LE value for the core layer. During the swelling process, the core layer tried to swell to its potential, but was restricted by the face layers. This action put the core layer in compression. As a reaction, the face layers were under tension in order for the specimen to be at an equilibrium stress state. The opposite was true for the perpendicular specimens as seen in the graph. The relatively flat stress distribution in the core layer for both parallel and perpendicular specimens was due to a gradual density decrease, which caused modulus decrease, towards the centerline of the sample. The effect of FWR on the magnitude of the swelling stresses is clearly seen in Fig. 7b. For a given exposure range (e.g., 35% to 93%RH), single-layer boards (FWR = 0 or 1) had relatively small swelling stresses across panel thickness. In these boards, the swelling stresses were caused mainly by the density gradient across panel thickness, which led to differential MCC and moduli between face and core layers. As soon as a certain portion of flakes was cross-laminated (i.e., three-layer structure), the swelling stresses increased significantly due to differential swelling potentials between cross-laminated flakes. The smaller the FWR, the larger the stresses at the face (tension for the parallel specimens and compression for the perpendicular specimens). For panels with smaller FWR values, only a small portion of the flakes was cross-laminated. During the swelling process, these flakes must react to a larger portion of the flakes oriented in the direction perpendicular to them having a different swelling potential. The action created swelling stresses of significant magnitude in the face layer. As FWR increased, the amount of flakes in the face layer became comparable to that in the core layer, which led to more balanced swelling stress distributions.

A typical instantaneous stress-strain relationship predicted by the model is shown in Fig. 8. The face flakes were aligned along the parallel direction and thus had smaller strains in the parallel direction. The core flakes were aligned along the perpendicular direction and

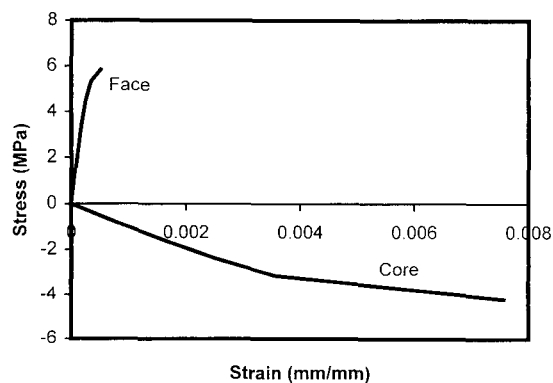


FIG. 8. Predicted instantaneous stress and strain relationship at the surface layer (a: face—0.5 mm deep from the surface and b: core—6.75 mm deep from the surface) for panels with FWR = 0.3 and RH change from 35% to 93%.

thus had larger swelling strains in the parallel direction. For the given FWR (i.e., 0.3) and RH exposure range (i.e., 35–93%), the stresses were large enough to cause instantaneous plastic deformation in both face and core layers. This indicates that a pure elastic approach would lead to a significant overestimate in the swelling stresses and underestimate in panel deformation for these panels. In all single-layer boards (FWR = 0 or 1), internal swelling stresses were not large enough to cause instantaneous plastic deformation in a given material direction, due to the similar swelling potentials among the layers across panel thickness. Thus, the stress-strain model adopted in this study was able to handle both linear and nonlinear conditions to provide an accurate prediction of in-plane stability behavior of OSB.

#### CONCLUSIONS

The in-plane stability behavior of three-layer OSB under varying environmental conditions was investigated through model analysis in the study. It was shown that PSR, LE, MOE, and MOR along both directions varied largely with panel processing variables. FAL and FWR were found to be the two primary factors for controlling in-plane bending and

swelling behavior of OSB at the RC levels used. LE followed a general curvilinear relationship with MC change, with a larger swelling rate at the lower MC ranges.

The predicted panel EM and LE as a function of FWR at various alignment and resin content levels demonstrated the balancing effect of cross-lamination, and the results agreed well with measured data. The predicted swelling stresses followed well-expected patterns, providing further insight into the complex swelling behavior of OSB. The model allows studying interactive influences of several processing variables including alignment level, flake weight ratio, and resin content. It provides an analytical tool for optimizing the balance between effective modulus and linear expansion for OSB manufacturing.

#### ACKNOWLEDGMENTS

This study was supported by the USDA National Research Initiative Competitive Grant Program (97-35103-5055). The financial contribution to the project is gratefully acknowledged.

#### REFERENCES

- AMERICAN SOCIETY FOR TESTING AND MATERIALS (ASTM). 1996. Annual book of ASTM standard D1037-96. American Society for Testing and Materials. Philadelphia, PA. 646 pp.
- BODIG, J., AND B. A. JAYNE. 1993. Mechanics of wood and wood composites. Krieger Publishing Company, Malabar, Florida. 712 pp.
- BRYAN, E. L. 1962. Dimensional stability of particleboard. *Forest Prod. J.* 12(12):572-576.
- GEIMER, R. L. 1982. Dimensional stability of flakeboards as affected by board specific gravity and flake alignment. *Forest Prod. J.* 32(8):44-52.
- HALLIGAN, A. F. 1970. A review of thickness swelling in particleboard. *Wood Sci. Technol.* 4(4):301-312.
- , AND A. P. SCHNIEWIND. 1974. Prediction of particleboard mechanical properties at various moisture contents. *Wood Sci. Technol.* 8(1):68-78.
- HSU, W. E. 1987. A process for stabilizing waferboard and OSB. Pages 219-236 in *Proc. 21th Washington State University International Symposium on Particleboard*. Pullman, WA.
- JOHNSON, J. W. 1964. Effect of exposure cycles on stability of commercial particleboard. *Forest Prod. J.* 14(7):277-282.
- JORGENSEN, R. N., AND R. L. ODELL. 1961. Dimensional stability of oak flakeboard as affected by particle geometry and resin spread. *Forest Prod. J.* 11(10):463-466.
- LANG, E. M., AND J. R. LOFERSKI. 1995. In-plane hygroscopic expansion of plywood and oriented strandboard. *Forest Prod. J.* 45(4):67-71.
- LAUFENBERG, T. L. 1983. Characterizing the nonlinear behavior of flakeboards. *Wood Fiber Sci.* 15(1):47-58.
- LEHMANN, W. F. 1978. Cyclic moisture conditions and their effect on strength and durability of structural flakeboards. *Forest Prod. J.* 28(6):23-31.
- LIU, J. Y., AND J. D. MCNATT. 1991. Thickness swelling and density variation in aspen flakeboards. *Wood Sci. Technol.* 25(1):73-82.
- REN, Y. 2000. Characterization of moisture sorption and thickness swelling behavior of oriented strandboard. Unpublished M.S. thesis, School of Forestry, Wildlife, and Fisheries, Louisiana State University. 84 pp.
- SUCHSLAND, O., AND H. XU. 1991. Model analysis of flakeboard variables. *Forest Prod. J.* 41(11/12):55-60.
- TALBOTT, J. W., T. M. MALONEY, E. M. HUFFCHER, R. J. HOYLE, AND R. W. MEYER. 1979. Analysis and design of COM\_PLY panels for dimensional stability as determined by interaction between the particleboard core and veneer facing components. Pages 25-82 in T. M. Maloney, ed. *Proc. 13th Washington State University International Symposium on Particleboard*. Pullman, WA.
- TANG, R. C., E. W. PRICE, AND C. C. CHEN. 1982. Hygroscopic effect on linear expansion of wood-based composites. Presentation at the National Meeting of the Society for Experimental Stress Analysis. Hawaii. 7 pp.
- , 1999. In-plane dimensional stability of oriented strandboard panel: Effect of processing variables. *Wood Fiber Sci.* 31(1):28-40.
- , AND M. R. MILOTA. 1995. Rheological behavior of Douglas-fir perpendicular to the grain at elevated temperatures. *Wood Fiber Sci.* 27(3):285-295.
- , AND O. SUCHSLAND. 1996. Linear expansion and its relationship to moisture content change for commercial oriented strand boards. *Forest Prod. J.* 46(11/12):79-83.
- , AND ———. 1997. Effect of moisture on the flexural properties of commercial oriented strandboards. *Wood Fiber Sci.* 29(1):47-57.
- , AND Y. REN. 2000. Characterization of sorption behavior of oriented strandboard under long-term cyclic exposure conditions. *Wood Fiber Sci.* 32(4):404-418.
- XU, W. 2000. Influence of percent alignment and shelling ratio on modulus of elasticity of oriented strandboard: a model investigation. *Forest Prod. J.* 50(10):43-47.
- , AND P. M. WINISTORFER. 1995. A procedure to determine thickness swelling distribution in wood composites panels. *Wood Fiber Sci.* 27(2):119-125.
- , AND O. SUCHSLAND. 1997. Linear expansion of wood composites: A model. *Wood Fiber Sci.* 29(3):272-281.

- , AND ———. 1998. Influence of out-of-plane orientation of particles on linear expansion of particleboard: A simulation study. *Forest Prod. J.* 48(6):85–87.
- ZYLKOWSKI, S. C. 1986. Dimensional stability of structural-use panels. American Plywood Assoc. Res. Report No. R & D 86L-43. Tacoma, WA. 16 pp.
- . 1989. Dimensional performance of wood-based siding. American Plywood Assoc. Res. Report No. 149. Tacoma, WA. 50 pp.